Structural Heart Disease

Patient-Specific Computer Simulation to Elucidate the Role of Contact Pressure in the Development of New Conduction Abnormalities After Catheter-Based Implantation of a Self-Expanding Aortic Valve

Giorgia Rocatello, MSc; Nahid El Faquir, MD; Gianluca De Santis, PhD;
Francesco Iannaccone, PhD; Johan Bosmans, MD, PhD; Ole De Backer, MD, PhD;
Lars Sondergaard, MD, DMSc; Patrick Segers, PhD; Matthieu De Beule, PhD;
Peter de Jaegere, MD, PhD*; Peter Mortier, PhD*

Background—The extent to which pressure generated by the valve on the aortic root plays a role in the genesis of conduction abnormalities after transcatheter aortic valve replacement (TAVR) is unknown. This study elucidates the role of contact pressure and contact pressure area in the development of conduction abnormalities after TAVR using patient-specific computer simulations.

Methods and Results—Finite-element computer simulations were performed to simulate TAVR of 112 patients who had undergone TAVR with the self-expanding CoreValve/Evolut R valve. On the basis of preoperative multi-slice computed tomography, a patient-specific region of the aortic root containing the atrioventricular conduction system was determined by identifying the membranous septum. Contact pressure and contact pressure index (percentage of area subjected to pressure) were quantified and compared in patients with and without new conduction abnormalities. Sixty-two patients (55%) developed a new left bundle branch block or a high-degree atrioventricular block after TAVR. Maximum contact pressure and contact pressure index (median [interquartile range]) were significantly higher in patients with compared with those without new conduction abnormalities (0.51 MPa [0.43–0.70 MPa] and 33% [22%–44%], respectively, versus 0.29 MPa [0.06–0.50 MPa] and 12% [1%–28%]). By multivariable regression analysis, only maximum contact pressure (odds ratio, 1.35; confidence interval, 1.1–1.7; *P*=0.01) and contact pressure index (odds ratio, 1.52; confidence interval, 1.1–2.1; *P*=0.01) were identified as independent predictors for conduction abnormalities, but not implantation depth.

Conclusions—Patient-specific computer simulations revealed that maximum contact pressure and contact pressure index are both associated with new conduction abnormalities after CoreValve/Evolut R implantation and can predict which patient will have conduction abnormalities. (*Circ Cardiovasc Interv*. 2018;11:e005344. DOI: 10.1161/CIRCINTERVENTIONS.117.005344.)

Key Words: aortic valve ■ atrioventricular block ■ computer simulation ■ regression analysis ■ tomography

Transcatheter aortic valve replacement (TAVR) is increasingly used to treat patients with severe aortic stenosis who are deemed inoperable or at high risk for surgical aortic valve replacement.[1] Recent clinical data demonstrate that TAVR is also a good alternative for surgical aortic valve replacement in intermediate-risk patients,[2] resulting in a further expansion of the indication for TAVR.[3]

At variance with surgical aortic valve replacement, conduction abnormalities (left bundle branch block [LBBB], high-degree atrioventricular block [AVB]) frequently occur after TAVR and remain a major clinical limitation as it may lead to permanent pacemaker implantation.[4]

Despite the fact that patient-, procedure-, and device-related variables have been shown to be associated with an increase of conduction abnormalities after TAVR, the underlying mechanism is not completely clear.[4] Some authors have mentioned that pressure generated by the prosthetic valve frame on the atrioventricular conduction pathway may be an important driver of new conduction abnormalities, although other mechanisms may play a role as well.[5–8]

Therefore, the aim of this study was to investigate to what extent mechanical pressure, assessed by patient-specific computer simulations, affects the conduction system after TAVR.

<div style="border:1px solid">

WHAT IS KNOWN

- Conduction abnormalities frequently occur during transcatheter aortic valve replacement as a result of (temporary or permanent) contact injury to the atrioventricular conduction tissue.
- The degree of injury most likely differs between patients and procedures.

WHAT THE STUDY ADDS

- The computational simulations performed in this study suggest that contact pressure and area subjected to contact pressure, but not the depth of valve implantation, are associated with the occurrence of new conduction abnormalities.

</div>

Methods

The data, analytic methods, and study materials will not be made available to other researchers for purposes of reproducing the results or replicating the procedure.

Study Population

The study population consists of 112 patients who underwent TAVR on native valves (ie, no valve-in-valve) using either the self-expanding CoreValve or an Evolut R transcatheter heart valve (Medtronic, MN) because of severe aortic stenosis (Table 1). All patients had undergone preoperative multi-slice computed tomography (MSCT) for sizing and that was of sufficient quality to allow computer simulation as previously described.[9,10] MSCT in-plane and through-plane resolution ranged from 0.32 to 0.97 mm/pixel, slice increment from 0.25 to 0.8 mm, and slice thickness from 0.5 to 1.5 mm.

This study was approved by the institutional review committee, and patients were selected for TAVR by the multidisciplinary Heart Team at the participating hospital. All patients were informed about the procedure and provided with informed written consent for the procedure and data collection.

Computer Simulations

Preoperative MSCT was used to generate patient-specific 3-dimensional models of the native aortic root anatomy that included the left ventricular outflow tract (LVOT), the calcified native leaflets, and the ascending aorta, using image segmentation techniques (Mimics v18.0; Materialise, Leuven, Belgium). The aortic wall and the leaflets were assumed to have a constant thickness of 2 mm and 1.5 mm, respectively.[9] Subsequently, virtual implantation of Medtronic CoreValve and CoreValve Evolut R systems in these aortic models was retrospectively performed using finite-element computer modeling (Abaqus/Explicit v6.12; Dassault Systèmes, Paris, France) as previously described.[9] In brief, CoreValve and CoreValve Evolut R frames were reconstructed from optical microscopy measurements and micro-computed tomography images, whereas the mechanical characteristics of the Nitinol frame were derived from in vitro radial compression tests at body temperature. The mechanical properties of the different tissues in the computer model were calibrated by an iterative back-calculation method using both pre- and postoperative MSCT images.[9] The aortic tissue was modeled with elastic material properties (E=2 MPa; v=0.45), and spring elements were added to incorporate the impact of surrounding structures in the model. The leaflets were assumed to be linear elastic (E=0.6 MPa; v=0.3), whereas calcifications were modeled using a stiffer elastic material with perfect plasticity (E=4 MPa; v=0.3; Yield stress=0.6 MPa). General contact with finite sliding between all the surfaces was applied with

Table 1. Characteristics of the Study Population

Parameters	All Patients (n=112)	Conduction Abnormalities		P Value
		Yes (n=62)	No (n=50)	
Baseline characteristics				
Female sex	56 (50)	31 (50)	25 (50)	>0.99
Age	82 [77–85]	83 [78.5–85]	80 [75.8–84]	0.12
EUROscore	12.2 [9.5–19.5]	12.6 [9.5–18.5]	11.7 [8.8–22.2]	0.94
Annular diameter, mm*	23.9±1.8	24.1±1.9	23.7±1.7	0.19
Height, cm	164.2±8.1	163.9±8.4	164.7±7.8	0.64
Weight, kg	71.9±12.1	72.0±12.5	71.7±11.8	0.92
BSA, m²	1.8±0.2	1.8±0.2	1.8±0.2	0.73
Pre–RBBB	5 (4)	3 (5)	2 (4)	0.83
IVS calcifications†	12 (11)	5 (8)	7 (14)	0.31
IBMS characteristics				
IBMS length, mm	10.2±3.7	10.5±3.9	9.8±3.3	0.29
IBMS angle, deg	18.8±15.2	19.6±14.7	17.7±15.9	0.52
p_1 depth, mm	5.5±3.2	5.2±3.5	5.8±2.9	0.32
p_3 depth, mm	2.2±2.4	1.7±2.2	2.8±2.5	0.02
Procedural characteristics				
Implantation depth, mm‡	7.2±3.5	8.4±3.2	5.8±3.2	<0.001
Device type				0.07
CoreValve (CV)	95 (85)	56 (90)	39 (78)	
Evolut R (CVER)	17 (15)	6 (10)	11 (22)	
Device size				0.37
CV26	30 (27)	17 (28)	13 (26)	
CV29	60 (54)	35 (57)	25 (50)	
CV31	5 (4)	4 (6)	1 (2)	
CVER26	6 (5)	2 (3)	4 (8)	
CVER29	11 (10)	4 (6)	7 (14)	
Sizing index§	1.18±0.1	1.17±0.1	1.19±0.1	0.29

Values are mean±SD, median [interquartile range] or n (%). BSA indicates body surface area; CV, CoreValve; CVER, CoreValve Evolut R; IBMS, inferior border of the membranous septum; IVS, interventricular septum; NCC, noncoronary cusp; and RBBB, right bundle branch block.

*Perimeter-based diameter=annular perimeter/π.

†Presence of calcifications in the IVS (plane perpendicular to the annulus).

‡Implantation depth assessed in postoperative angiograms: distance from the aortic annular plane on the NCC side to the deepest level of the most proximal edge of the device frame.

§Sizing index=(device size)/(perimeter-based diameter).

hard contact properties to prevent penetrations along the normal direction. A friction coefficient of 0.7 was used to model the interaction between the frame and the aortic model.

These computer simulations allow to assess device–host interaction and, thus, device and aortic wall deformation and the resulting contact pressure exerted by the frame on the surrounding anatomy. During the computer simulations, all steps of the clinical implantation consisting of pre-dilatation (ie, balloon size), valve size, depth
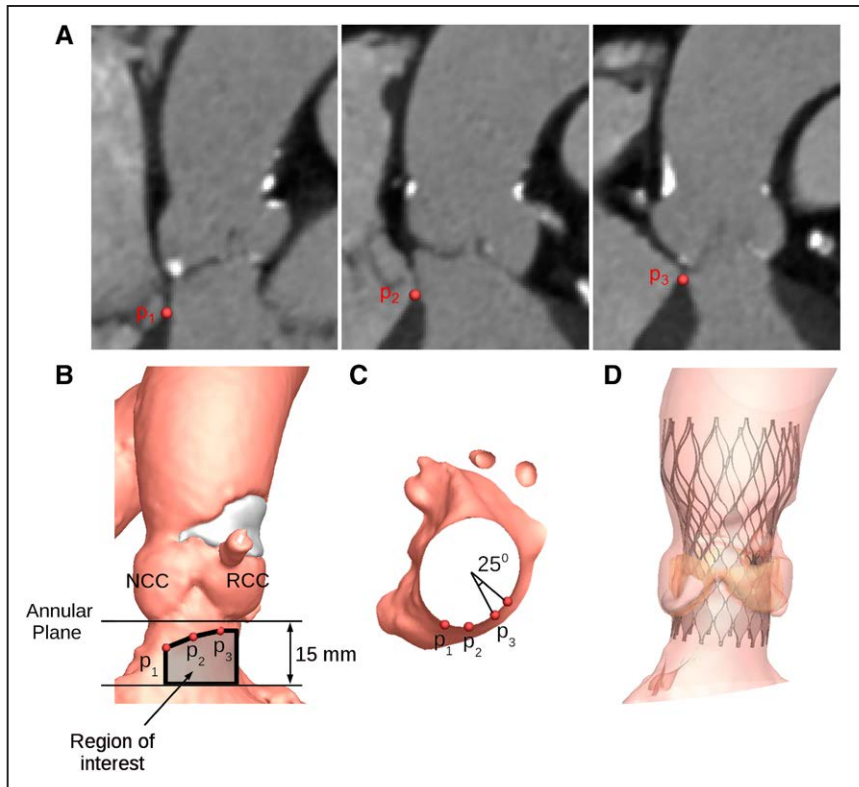
Figure 1. Identification of anatomic landmarks and computer modeling workflow. **A**, Identification of inferior border of the membranous septum (IBMS) in the preoperative multi-slice computed tomography (MSCT) images through 3 consecutive landmarks (p_1, p_2, p_3, in red); (**B**, **C**) patient-specific 3-dimensional aortic model with, in black, the selected region of interest in vicinity of the atrioventricular conduction system from a frontal view (**B**) and from a top view (**C**); (**D**) virtual implantation of the Medtronic CoreValve device at the same implantation depth as done in the real procedure. NCC indicates noncoronary cusp; and RCC, right coronary cusp.

of implantation, and post-dilatation (ie, balloon size) if applied were respected, as previously described in 2 studies in which the software was validated for the assessment of frame geometry and expansion, calcium displacement, and paravalvular leakage.[9,10] Device repositioning of the Evolut R was not integrated in the model, but the final depth of implantation at the noncoronary cusp (NCC) and left coronary cusp was matched with the actual depth of implantation derived from contrast angiography performed immediately after TAVR, using the same projection angle.

Pressure Analysis

From each finite-element simulation, the force exerted on the recipient anatomy was extracted. For the purpose of this study (ie, relationship between contact pressure and new conduction abnormalities after TAVR), the region of the LVOT that contains the atrioventricular conduction system was defined as the region of interest. At that region, (1) maximum contact pressure and (2) contact pressure index (ie, the percentage of this region of interest subjected to contact pressure) were calculated (Figures 1, 2, and 3).

The region of interest for the contact pressure analysis was selected on each 3-dimensional aortic root model, starting from the inferior border of the membranous septum (IBMS), as this represents an

anatomic surrogate for the surfacing of the His bundle and the transition to the left bundle branch.[11–13] To identify the IBMS, 3 dedicated landmarks were determined on the preoperative MSCT images at the transition between the interventricular membranous septum (MS) and muscular septum[14] in the resliced view perpendicular to the annular plane (Figure 1). Two of these landmarks were selected at the beginning and at the end of the IBMS, namely p_1 and p_3, with p_1 closer to the NCC and p_3 closer to the right coronary cusp (RCC). An additional point (p_2) was selected in between to better track the course of the IBMS as this is often not a straight line (Figure 1A). If an abrupt change in the IBMS was seen when scrolling through the MSCT images between p_1 and p_3, p_2 was chosen at that location. On the basis of anatomic findings,[11,15] the region of interest for the contact pressure analysis was defined by the area between the IBMS (extended toward the RCC by a 25° angle) and the plane 15 mm below the annulus (Figure 1B and 1C), to ensure the inclusion of the proximal part of the left bundle branch.

The effect of frame rotation on contact pressure and contact pressure index was taken into account by simulating for each patient 3 different rotations of the frame: starting from a reference position the frame was rotated with 6° and 12°. The resulting maximum contact pressure and contact pressure index for these different rotations were then averaged per patient.
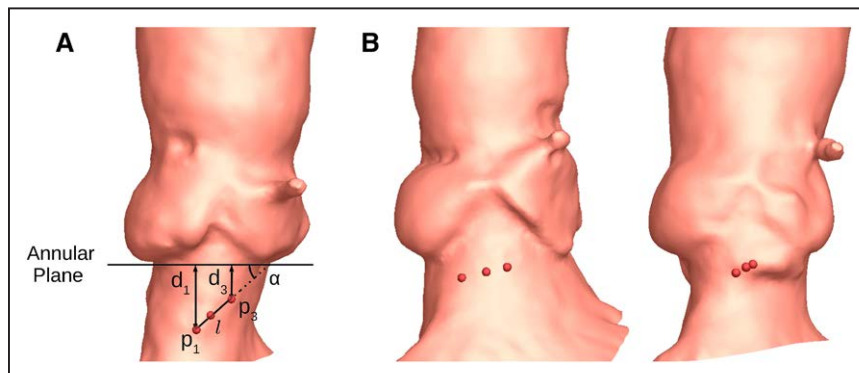

Figure 2. Anatomic variability—IBMS is represented by 3 red landmarks. **A**, Illustration of the inferior border of the membranous septum (IBMS)–related anatomic measurements: IBMS length (l)—distance between landmarks p_1 and p_3, IBMS location (d_1 and d_3)—distance of landmarks p_1 and p_3 from the annular plane, IBMS orientation (α)—angle between the segment connecting p_1 and p_3 and the annular plane. **B**, Representative illustration of IBMS identification in 2 patients.

Table 2. Simulation Results

Parameters	All Patients (n=112)	Conduction Abnormalities		P Value
		Yes (n=62)	No (n=50)	
Maximum pressure [MPa]	0.46 [0.26–0.62]	0.51 [0.43–0.70]	0.29 [0.06–0.50]	<0.001
Contact pressure index [%]	26 [13–40]	33 [22–44]	12 [1–28]	<0.001

Values are mean±SD, median [interquartile range] or n (%).

Besides the contact pressure analysis, the anatomic variability of the length, location, and orientation of the IBMS was investigated (Figure 2A). The length of the IBMS (l) was defined as the distance between the first (p_1) and the last (p_3) selected landmarks, the location of the IBMS was defined as the relative distance of points p_1 (d_1) and p_3 (d_3) to the aortic annular plane, and the orientation of the IBMS was described by the angle α between the segment connecting p_1 and p_3, and the aortic annular plane.

Statistical Analysis

Continuous variables are expressed as mean±SD or median [interquartile range], stratified by the occurrence of new TAVR-related conduction abnormalities, and compared using the Student *t* test or Mann–Whitney–Wilcoxon test depending on the variable distribution. Discrete variables are expressed as percentage and compared using the χ^2 or the Fisher exact test where appropriate. The nonparametric Friedman test was used to analyze differences in maximum contact pressure and contact pressure index between 3 different rotations of the device. Anatomic baseline characteristics and procedural parameters that were considered relevant for the development of conduction abnormalities were analyzed together with the maximum contact pressure and contact pressure index. Only variables yielding a *P* value <0.1 in the univariable analysis were included in the stepwise logistic regression (backward likelihood ratio) analysis. Only for significant results (*P*<0.05), receiver-operating characteristics curves were generated to find optimal cutoff values (Youden index criterion[16]), and sensitivity, specificity, positive predictive value, negative predicted value, and accuracy were calculated. Correlation between implantation depth, maximum contact pressure and contact pressure index was also analyzed, and results are reported in the Data Supplement. Statistical analysis was performed with the statistical software package SPSS version 22.0 (IBM Corporation, New York).

Results

Baseline patient- and procedure-related characteristics are summarized in Table 1. Sixty-two patients (55%) developed new conduction abnormalities after TAVR: LBBB or high-degree AVB (second-degree AVB Mobitz 2 or third-degree

AVB). A higher number of patients developed new conduction abnormalities after implantation of a CoreValve compared with those who received an Evolut R (59% versus 35%). There were no other differences between patients with and without a new conduction abnormality, except for a deeper implantation of the valve in the LVOT (8.4 versus 5.8 mm; *P*<0.001) and a more shallow position of the IBMS at p_3 (1.7 versus 2.8 mm) in the group with conduction abnormalities. An example of the variations in anatomy of the IBMS is illustrated in Figure 2.

Contact Pressure on the LVOT in the Region of Interest

The nonparametric Friedman test showed no statistical difference in maximum contact pressure and contact pressure index between the 3 device rotations (*P*=0.073 and *P*=0.698, respectively). Maximum pressure and contact pressure index were both significantly higher in patients with a new conduction abnormality after TAVR (*P*<0.001; Table 2). The median value of maximum contact pressure (0.51 MPa [0.43–0.70 MPa]) and contact pressure index (33% [22%–44%]) was 2- to 3-fold higher in patients with a new conduction abnormality compared with patients without a new conduction abnormality (0.29 MPa [0.06–0.50 MPa] and 12% [1%–28%]; Figure 4). In the majority of patients (89%), the maximum contact pressure was observed in the upper half of the region of interest.

Computer simulation results in a patient without and with a new conduction abnormality with comparable depth of implantation of the device are shown in Figure 3. In the patient without a new conduction abnormality, a low maximum contact pressure (≤0.11 MPa) in the vicinity of the conduction system (region of interest delimited by the black border) was observed. Conversely, the patient who developed a new AVB
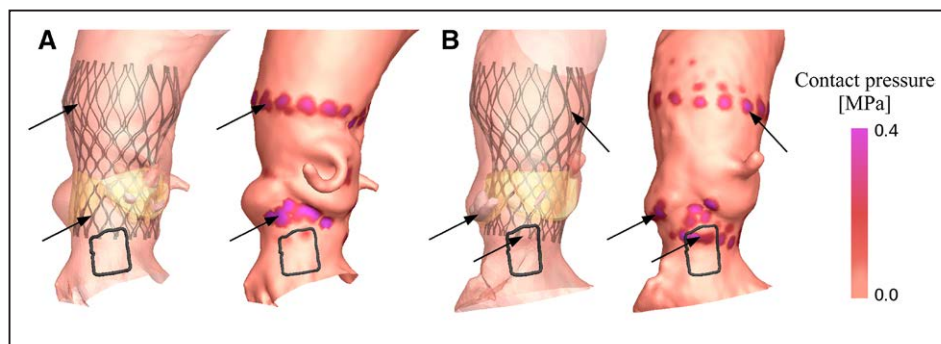

Figure 3. Contact pressure: representative examples. Representative example of contact pressure observed on the aortic root areas where the aortic root is in contact and interacts with calcifications and device frame (indicated by black arrows). The region of interest is delimited by the black line. **A**, Case without a new transcatheter aortic valve replacement (TAVR)–induced conduction abnormality: maximum contact pressure=0.11 MPa and contact pressure index=20%. **B**, Case with new TAVR-induced high-degree atrioventricular block (AVB): maximum contact pressure=0.85 MPa, and contact pressure index=29%.
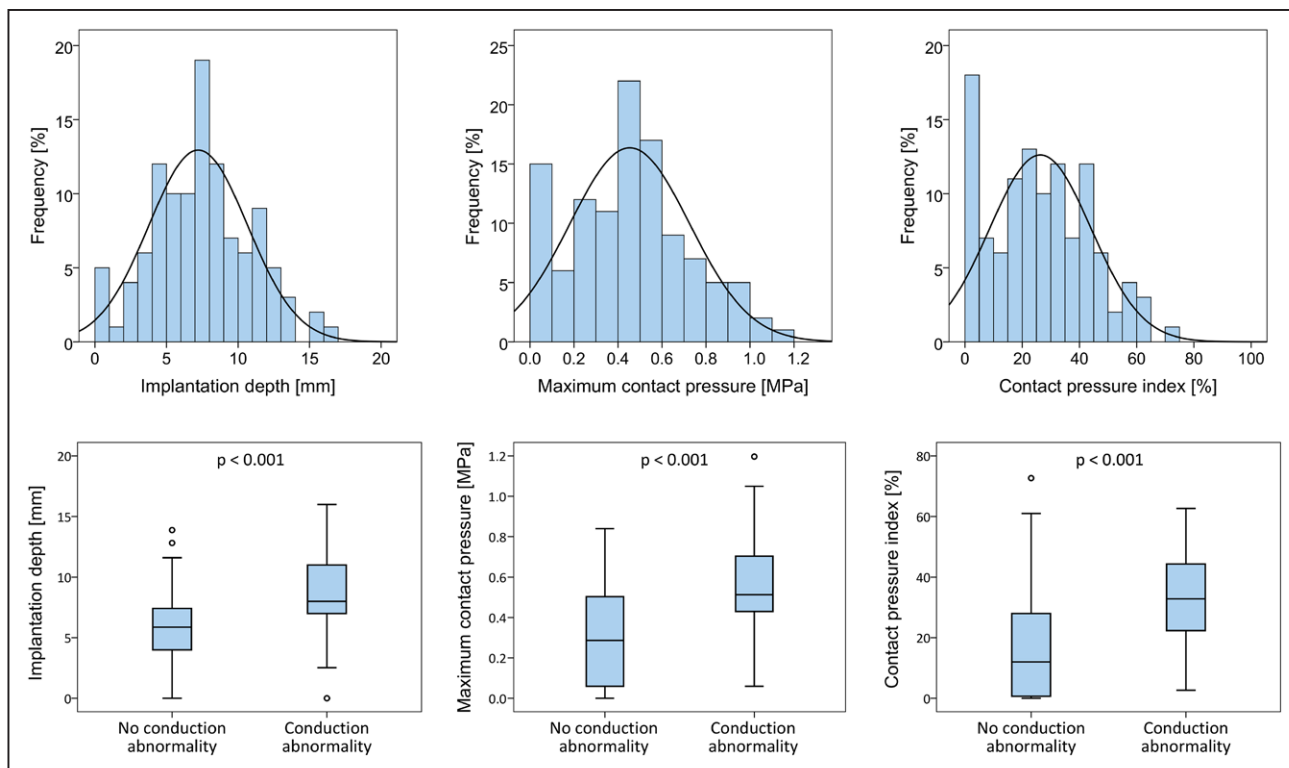
Figure 4. Histograms and box plot diagrams of valve implantation depth, maximum contact pressure, and contact pressure index. **Upper**, Distribution of valve implantation depth (**left**), maximum contact pressure (**middle**), and contact pressure index (**right**) in comparison to a normal probability curve (black curve). **Lower**, Box plot diagrams of valve implantation depth (*P*<0.001, **left**), maximum contact pressure (*P*<0.001, **middle**), and contact pressure index (*P*<0.001, **right**) in patients with and without conduction abnormalities. Extreme values are presented as small circles (o).

experienced high contact pressure within the region of interest (up to 0.85 MPa) and an extended area of contact (contact pressure index of 29%).

Interestingly, not all the models showed contact between the valve frame and the region of interest. Figure 5 illustrates 3 patients where no contact was observed in the region of interest because of a large calcium nodule precluding apposition of the frame (Figure 5A), of an anatomic low position of the IBMS (Figure 5B), and of a large LVOT resulting in malapposition of the frame (Figure 5C).

The multivariable regression analysis identified maximum contact pressure (odds ratio, 1.35; confidence interval, 1.1–1.7; *P*=0.01) and contact pressure index (odds ratio, 1.52; confidence interval, 1.1–2.1; *P*=0.01) as the only independent predictors of conduction abnormalities (Table 3).

Receiver-operating characteristics curve analysis (Figure 6) revealed an area under the curve of 0.76 and 0.79 for maximum contact pressure and contact pressure index, respectively. A cutoff value of 0.39 MPa for the maximum contact pressure ensured a sensitivity, specificity, positive predictive value, negative predicted value, and accuracy of 85%, 64%, 75%, 78% and 76%, respectively. This was 95%, 54%, 72%, 90%, and 77%, respectively, for a contact pressure index of 14%. The accuracy of prediction was further increased when combining both contact pressure parameters (Figure 7). Fifty-three patients (79%) with a maximum contact pressure >0.39 MPa and a contact pressure index >14% developed a new conduction abnormality. In case of a maximum contact

pressure <0.39 MPa and a contact pressure index <14%, 23 patients (88%) did not experience new conduction abnormalities. Four patients with a maximum contact pressure >0.39 MPa and a contact pressure index <14% (ie, small area of high contact pressure) did not develop conduction abnormalities, whereas 6 patients (40%) with a low maximum contact pressure and contact pressure index >14% developed new conduction abnormalities.

Discussion

The main goal of this study was to investigate the relation between the mechanical pressure generated by the prosthetic valve frame on the aortic root at the site of the atrioventricular conduction tissue and the development of new conduction abnormalities after TAVR. Using patient-specific computer simulations, maximum contact pressure and contact pressure index were both assessed. The impact of device rotation on the contact pressure within the region of interest was also evaluated, but no significant difference on the variations of both parameters because of the device rotations was observed. Both simulation-based parameters were associated with new conduction abnormalities (LBBB and high-degree AVB) after implantation of a self-expanding valve. Of note, the multivariable analysis indicated that contact pressure, but not implantation depth, is the driving force of the development of new conduction abnormalities. Yet it remains difficult to elucidate whether pressure levels or relative area is the overriding factor. In addition, cutoff values were identified
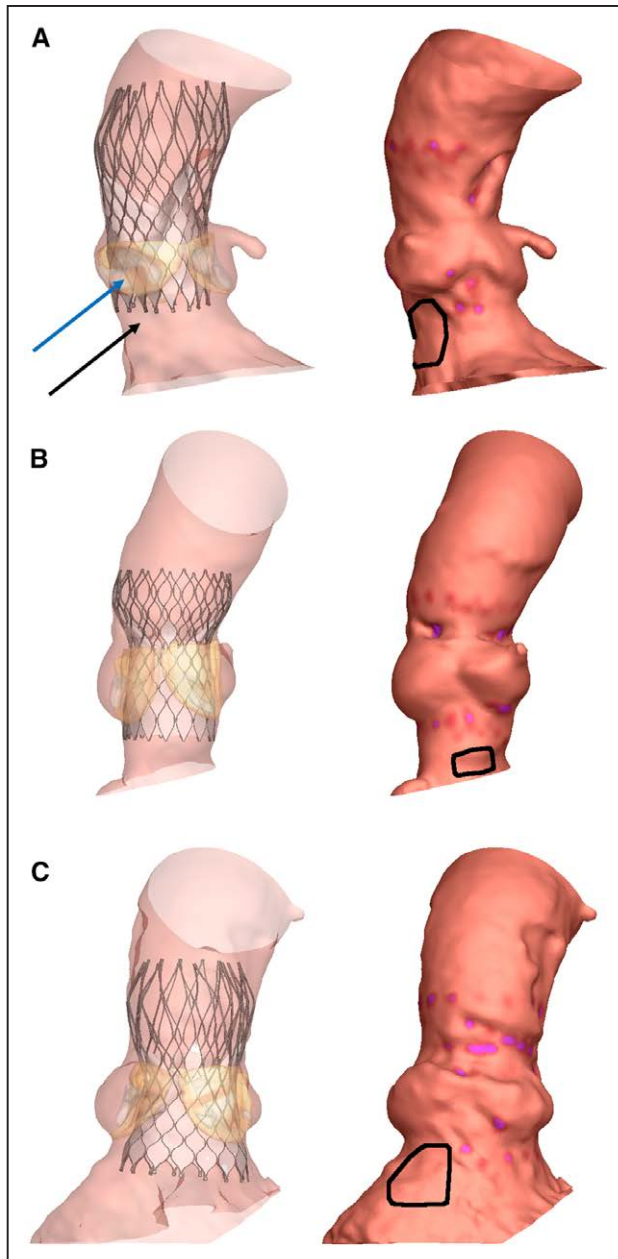
Figure 5. Representative cases with no contact within the region of interest. **A**, Large valve calcification (blue arrow) that determines underexpansion of the frame (black arrow); (**B**) anatomic low position of the inferior border of the membranous septum (IBMS); (**C**) large left ventricular outflow tract (LVOT) and bad apposition of the valve frame with the aortic wall.

Table 3. Results of the Logistic Regression for Association With Post-Transcatheter Aortic Valve Replacement Conduction Abnormalities

Parameters	Univariable P Value	Multivariable Analysis P Value	Odds Ratio	95% CI
p_3 depth, mm	0.017	…	…	…
Device type	0.071	…	…	…
Implantation depth, mm	<0.001	…	…	…
Maximum pressure, MPa	<0.001	0.010	1.35	1.1–1.7
Contact pressure index, %	<0.001	0.013	1.52	1.1–2.1

CI indicates confidential interval.

length of the IBMS. In our analysis, the IBMS was located below the annular plane on the NCC side and extended toward the RCC. In about 13% of the cases, the landmark p_3 was found to be superior to the annular plane, meaning that the distal part of the IBMS intersected the interleaflet triangle between NCC and RCC. A representative example is shown in Figure 8. These findings are in accordance with those of Kawashima and Sato[15] (2014) who also found the MS to be located between the NCC and the RCC (frequently located on the RCC side), with reaching the annular plane in about 80% of the cases. Irrespective to the interindividual variability of the precise relationship between the MS and the conduction tissue, this area is susceptible to injury during TAVR. In particular, the position of the IBMS at the RCC side (depth of p_3) was found to be inversely associated with risk of new conduction abnormalities; however, the multivariable analysis did not show it to be an independent predictor of new conduction abnormalities.

Several studies consistently revealed the relation between a too deep implantation of the prosthesis and the occurrence of new-onset LBBB and permanent pacemaker implantation.[17–21] In our study, such correlation emerged in the univariable analysis, but it did not show to be statistically significant in the subsequent multivariable analysis. The findings of this study are not in disagreement with those who focused on the role of depth of implantation because this study incorporated both depth of implantation and contact pressure and contact pressure area. Depth of implantation and area of contact pressure are intrinsically related to one another. This study merely indicates that the degree of pressure and area of contact pressure are more important than the depth of implantation by itself, which is from a pathophysiologic perspective a logic finding. Although a high implantation is nowadays recommended to avoid conduction abnormalities, the findings of this study indicate that the optimal implantation depth is patient specific given the anatomic variability of the MS. General implantation depth guidelines may not lead to the best clinical outcome for each individual. This is in agreement with the recent work of Hamdan et al[14] who identified the 2-dimensional MSCT-based distance from the IBMS to the annular plane and the difference between this parameter and the device implantation depth as predictors of high-degree AVB and permanent pacemaker implantation. The results of our anatomic
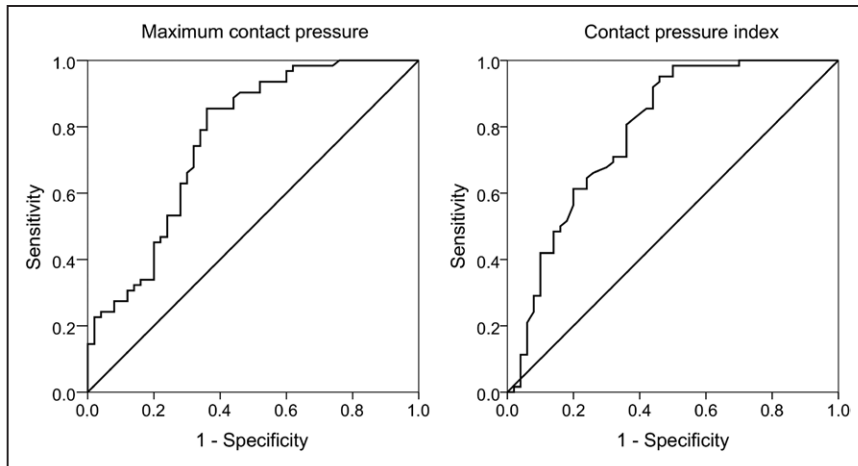
that could discern patients who did and did not develop new conduction abnormalities after TAVR.

On the basis of the preoperative MSCT, anatomic landmarks were identified to define a patient-specific region on the LVOT in which the contact pressure was evaluated. The definition of this region is based on the consideration that the His bundle is located at (or slightly below) the transition between the interventricular MS and muscular septum in at least 80% of the cases.[13] Three-dimensional measurements of the IBMS revealed large anatomic variability within the studied population in terms of location, orientation, and

Figure 6. Receiver-operator characteristics (ROC) curves of maximum contact pressure and contact pressure index. ROC curve analysis of maximum contact pressure (area under the curve [AUC]=0.76, **left**) and contact pressure index (AUC=0.79, **right**).

analysis of the IBMS (eg, the distance from the IBMS to the annular plane varies the course of the IBMS) indicate, however, that a single 2-dimensional measurement may not fully describe this structure.

Given the above and in line with the demand from society and authorities to move to patient-specific treatment to enhance safety and efficacy of treatment, thereby, reducing costs, this and previous works on computer simulations indicate the role of patient-specific computer simulations in the planning of TAVR offering the physician to choose the valve size that best fits the individual patient in addition to the optimal depth of implantation.[22,23] The findings of this study indicate that patient-specific computer simulation pre-TAVR may identify which patient will develop a new conduction abnormality. Previous works indicated the reliability of specific computer simulation in the prediction of the presence and severity of paravalvular leakage.[10] Both outcome measures can currently be assessed and quantified during the same

simulation and may, thus, help the physician to choose the valve that best fits the individual patient.

Study Limitations
The results of this study only relate to the self-expanding CoreValve and Evolut R valves. Its applicability to other transcatheter aortic valve systems currently in use should be confirmed. Also the effect of device repositioning was not taken into account; however, it may be hypothesized that especially the final implantation depth is the most determining factor for inducing conduction abnormalities. Linear elastic material properties were used to model the aortic tissue. Although the hyperelastic model better reflects actual tissue behavior, the used material parameters accurately predict interactions between the aorta and the TAVR device, as previously demonstrated.[9,24] Future studies should be performed to validate the cutoffs identified to discriminate between patients who did and did not develop a new conduction abnormality. Furthermore, it might be interesting to investigate the predictive power of maximum contact pressure and contact pressure index with respect to the type of disturbance (LBBB or AVB). Finally, a further quantitative analysis of the location of the maximum contact pressure within the region of interest during the entire cardiac cycle may offer a better insight in the mechanisms of the development of new conduction abnormalities after TAVR.

Conclusions
Patient-specific computer simulations revealed that maximum contact pressure and contact pressure index are associated with new conduction abnormalities after CoreValve/Evolut R implantation and can predict which patient will have a conduction abnormality after TAVR.
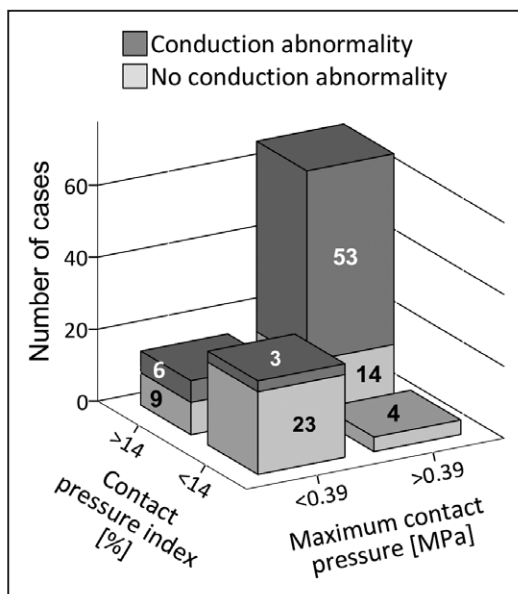
Figure 7. Prediction of conduction abnormalities according to the maximum contact pressure and contact pressure index. Prediction of conduction abnormalities according to the maximum contact pressure and contact pressure index based on the chosen cutoff values (0.39 MPa and 14%, respectively).
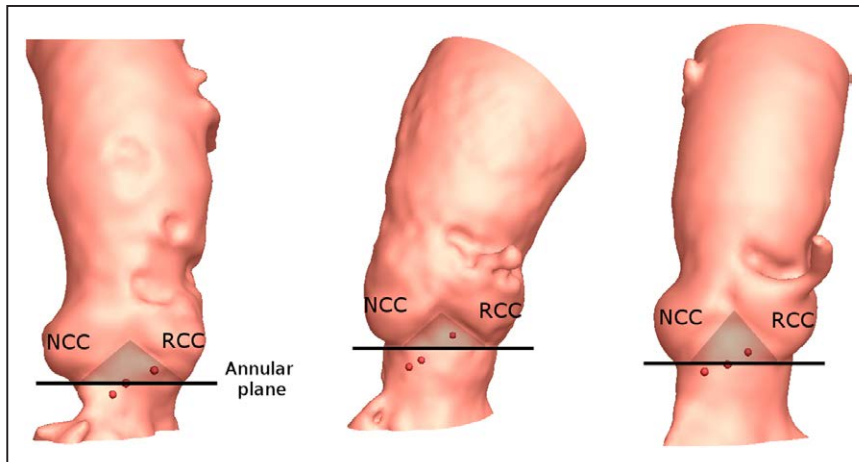
Figure 8. Representative examples of high inferior border of the membranous septum (IBMS). Three patients where the IBMS (red rots) was found to end superiorly to the annular plane (black line) and thus intersecting the interleaflet triangle between noncoronary cusp (NCC) and right coronary cusp (RCC; light grey zone).

Disclosures

References

1. Mylotte D, Osnabrugge RLJ, Windecker S, Lefevre T, de Jaegere P, Wenaweser P, Maisano F, Moat N, Sondergaard L, Campante Teles R, Martucci G, Manoharan G, Garcia E, Van Mieghem NM, Kappetein AP, Serruys PW, Lange R, Piazza N. TCT-752 transcatheter aortic valve replacement in Europe: the 2013 update. *JACC Cardiovasc Interv*. 2013;62:B229.

2. Leon MB, Smith CR, Mack MJ, Makkar RR, Svensson LG, Kodali SK, Thourani VH, Tuzcu EM, Miller DC, Herrmann HC, Doshi D, Cohen DJ, Pichard AD, Kapadia S, Dewey T, Babaliaros V, Szeto WY, Williams MR, Kereiakes D, Zajarias A, Greason KL, Whisenant BK, Hodson RW, Moses JW, Trento A, Brown DL, Fearon WF, Pibarot P, Hahn RT, Jaber WA, Anderson WN, Alu MC, Webb JG; PARTNER 2 Investigators. Transcatheter or surgical aortic-valve replacement in intermediate-risk patients. *N Engl J Med*. 2016;374:1609–1620. doi: 10.1056/NEJMoa1514616.

3. Thourani VH, Kodali S, Makkar RR, Herrmann HC, Williams M, Babaliaros V, Smalling R, Lim S, Malaisrie SC, Kapadia S, Szeto WY, Greason KL, Kereiakes D, Ailawadi G, Whisenant BK, Devireddy C, Leipsic J, Hahn RT, Pibarot P, Weissman NJ, Jaber WA, Cohen DJ, Suri R, Tuzcu EM, Svensson LG, Webb JG, Moses JW, Mack MJ, Miller DC, Smith CR, Alu MC, Parvataneni R, D'Agostino RB, Jr, Leon MB. Transcatheter aortic valve replacement versus surgical valve replacement in intermediate-risk patients: a propensity score analysis. *Lancet*. 2016;387:2218–2225. doi: 10.1016/S0140-6736(16)30073-3.

4. van der Boon RM, Nuis RJ, Van Mieghem NM, Jordaens L, Rodés-Cabau J, van Domburg RT, Serruys PW, Anderson RH, de Jaegere PP. New conduction abnormalities after TAVI–frequency and causes. *Nat Rev Cardiol*. 2012;9:454–463. doi: 10.1038/nrcardio.2012.58.

5. Houthuizen P, Van Garsse LA, Poels TT, de Jaegere P, van der Boon RM, Swinkels BM, Ten Berg JM, van der Kley F, Schalij MJ, Baan J, Jr, Cocchieri R, Brueren GR, van Straten AH, den Heijer P, Bentala M, van Ommen V, Kluin J, Stella PR, Prins MH, Maessen JG, Prinzen FW. Left bundle-branch block induced by transcatheter aortic valve implantation increases risk of death. *Circulation*. 2012;126:720–728. doi: 10.1161/CIRCULATIONAHA.112.101055.

6. Morís C, Rubín JM. Conduction disorders and transcatheter aortic valve. Clinically relevant or just a mild complication? *Rev Esp Cardiol (Engl Ed)*. 2013;66:692–694. doi: 10.1016/j.rec.2013.05.006.

7. Bax JJ, Delgado V, Bapat V, Baumgartner H, Collet JP, Erbel R, Hamm C, Kappetein AP, Leipsic J, Leon MB, MacCarthy P, Piazza N, Pibarot P, Roberts WC, Rodés-Cabau J, Serruys PW, Thomas M, Vahanian A, Webb J, Zamorano JL, Windecker S. Open issues in transcatheter aortic valve implantation. Part 2: procedural issues and outcomes after transcatheter aortic valve implantation. *Eur Heart J*. 2014;35:2639–2654. doi: 10.1093/eurheartj/ehu257.

8. Nuis RJ, Van Mieghem NM, Schultz CJ, Tzikas A, Van der Boon RM, Maugenest AM, Cheng J, Piazza N, van Domburg RT, Serruys PW, de Jaegere PP. Timing and potential mechanisms of new conduction abnormalities during the implantation of the Medtronic CoreValve System in patients with aortic stenosis. *Eur Heart J*. 2011;32:2067–2074. doi: 10.1093/eurheartj/ehr110.

9. Schultz C, Rodriguez-Olivares R, Bosmans J, Lefèvre T, De Santis G, Bruining N, Collas V, Dezutter T, Bosmans B, Rahhab Z, El Faquir N, Watanabe Y, Segers P, Verhegghe B, Chevalier B, van Mieghem N, De Beule M, Mortier P, de Jaegere P. Patient-specific image-based computer simulation for the prediction of valve morphology and calcium displacement after TAVI with the Medtronic CoreValve and the Edwards SAPIEN valve. *EuroIntervention*. 2016;11:1044–1052. doi: 10.4244/EIJV11I9A212.

10. de Jaegere P, De Santis G, Rodriguez-Olivares R, Bosmans J, Bruining N, Dezutter T, Rahhab Z, El Faquir N, Collas V, Bosmans B, Verhegghe B, Ren C, Geleinse M, Schultz C, van Mieghem N, De Beule M, Mortier P. Patient-specific computer modeling to predict aortic regurgitation after transcatheter aortic valve replacement. *JACC Cardiovasc Interv*. 2016;9:508–512. doi: 10.1016/j.jcin.2016.01.003.

11. Massing GK, James TN. Anatomical configuration of the His bundle and bundle branches in the human heart. *Circulation*. 1976;53:609–621.

12. Piazza N, de Jaegere P, Schultz C, Becker AE, Serruys PW, Anderson RH. Anatomy of the aortic valvar complex and its implications for transcatheter implantation of the aortic valve. *Circ Cardiovasc Interv*. 2008;1:74–81. doi: 10.1161/CIRCINTERVENTIONS.108.780858.

13. Kawashima T, Sasaki H. Gross anatomy of the human cardiac conduction system with comparative morphological and developmental implications for human application. *Ann Anat*. 2011;193:1–12. doi: 10.1016/j.aanat.2010.11.002.

14. Hamdan A, Guetta V, Klempfner R, Konen E, Raanani E, Glikson M, Goitein O, Segev A, Barbash I, Fefer P, Spiegelstein D, Goldenberg I, Schwammenthal E. Inverse relationship between membranous septal length and the risk of atrioventricular block in patients undergoing transcatheter aortic valve implantation. *JACC Cardiovasc Interv*. 2015;8:1218–1228. doi: 10.1016/j.jcin.2015.05.010.

15. Kawashima T, Sato F. Visualizing anatomical evidences on atrioventricular conduction system for TAVI. *Int J Cardiol*. 2014;174:1–6. doi: 10.1016/j.ijcard.2014.04.003.

16. Youden WJ. Index for rating diagnostic tests. *Cancer*. 1950;3:32–35.

17. Piazza N, Nuis RJ, Tzikas A, Otten A, Onuma Y, García-García H, Schultz C, van Domburg R, van Es GA, van Geuns R, de Jaegere P, Serruys PW. Persistent conduction abnormalities and requirements for pacemaking six months after transcatheter aortic valve implantation. *EuroIntervention*. 2010;6:475–484. doi: 10.4244/EIJ30V6I4A80.

18. Urena M, Mok M, Serra V, Dumont E, Nombela-Franco L, DeLarochellière R, Doyle D, Igual A, Larose E, Amat-Santos I, Côté M, Cuéllar H, Pibarot P, de Jaegere P, Philippon F, Garcia del Blanco B, Rodés-Cabau J. Predictive factors and long-term clinical consequences of persistent left bundle branch block following transcatheter aortic valve implantation with a balloon-expandable valve. *J Am Coll Cardiol*. 2012;60:1743–1752. doi: 10.1016/j.jacc.2012.07.035.

19. Mouillet G, Lellouche N, Lim P, Meguro K, Yamamoto M, Deux JF, Monin JL, Bergoënd E, Dubois-Randé JL, Teiger E. Patients without prolonged QRS after TAVI with CoreValve device do not experience high-degree

atrio-ventricular block. *Catheter Cardiovasc Interv*. 2013;81:882–887. doi: 10.1002/ccd.24657.

20. Pereira E, Ferreira N, Caeiro D, Primo J, Adão L, Oliveira M, Gonçalves H, Ribeiro J, Santos E, Leite D, Bettencourt N, Braga P, Simões L, Vouga L, Gama V. Transcatheter aortic valve implantation and requirements of pacing over time. *Pacing Clin Electrophysiol*. 2013;36:559–569. doi: 10.1111/pace.12104.

21. Lenders GD, Collas V, Hernandez JM, Legrand V, Danenberg HD, den Heijer P, Rodrigus IE, Paelinck BP, Vrints CJ, Bosmans JM. Depth of valve implantation, conduction disturbances and pacemaker implantation with CoreValve and CoreValve Accutrak system for Transcatheter Aortic Valve Implantation, a multi-center study. *Int J Cardiol*. 2014;176:771–775. doi: 10.1016/j.ijcard.2014.07.092.

22. Smith N, de Vecchi A, McCormick M, Nordsletten D, Camara O, Frangi AF, Delingette H, Sermesant M, Relan J, Ayache N, Krueger MW, Schulze WH, Hose R, Valverde I, Beerbaum P, Staicu C, Siebes M, Spaan J, Hunter P, Weese J, Lehmann H, Chapelle D, Rezavi R. euHeart: personalized and integrated cardiac care using patient-specific cardiovascular modelling. *Interface Focus*. 2011;1:349–364. doi: 10.1098/rsfs.2010.0048.

23. Kirchhof P, Sipido KR, Cowie MR, Eschenhagen T, Fox KA, Katus H, Schroeder S, Schunkert H, Priori S; ESC CRT R&D and European Affairs Work Shop on Personalized Medicine. The continuum of personalized cardiovascular medicine: a position paper of the European Society of Cardiology. *Eur Heart J*. 2014;35:3250–3257. doi: 10.1093/eurheartj/ehu312.

24. Russ C, Hopt R, Sundermann S, Falk V, Szekely G, Gessat M. Simulation of transcatheter aortic valve implantation under consideration of leaflet calcification. Paper presented at: 35th Annual International Conference of IEEE EMBS; Osaka, Japan; July 3–7, 2018. http://ieeexplore.ieee.org/document/6609599/. Accessed January 15, 2018.